Tanshinone IIA induces cytochrome *c*-mediated caspase cascade apoptosis in A549 human lung cancer cells via the JNK pathway

JIAN ZHANG[1], JU WANG[1], JIU-YANG JIANG[1], SHANG-DIAN LIU[2], KAI FU[1] and HONG-YU LIU[2]

Departments of [1]Thoracic Surgery and [2]Cardiovascular Surgery, The First Affiliated Hospital, Harbin Medical University, Harbin 150001, P.R. China

Received March 20, 2014; Accepted May 14, 2014

DOI: 10.3892/ijo.2014.2471

Abstract. Tanshinone IIA (TSIIA), a natural diterpene quinone in the traditional Chinese medicinal herb Dan-Shen (*Salvia miltiorrhiza*), has extensively exerted antitumor activity in cellular and animal models. However, the molecular mechanisms underlying the antitumor effects of TSIIA remain largely unknown. The *in vitro* effects of TSIIA on apoptosis were investigated in A549 non-small cell lung cancer (NSCLC) cells. The data showed that TSIIA significantly suppressed the proliferation of A549 cells in a dose-dependent manner, with IC_{50} values of 16.0±3.7 and 14.5±3.3 μM at 48 h as determined by Cell Counting Kit-8 (CCK-8) assay and clone formation assay, respectively. The change of mitochondrial morphology and the loss of mitochondrial membrane potential (MMP) were observed during the induction. Furthermore, TSIIA induced A549 cell apoptosis as confirmed by typical morphological changes, with cytochrome *c* release from the mitochondria and Bax translocation to the mitochondria. Caspase activity data indicated that TSIIA activated caspase-9 and caspase-3 of mitochondria-mediated apoptosis, but not caspase-8 of receptor-mediated apoptosis, which could be largely rescued by SP600125 (JNK inhibitor). Taken together, these findings provide the first evidence that TSIIA inhibits growth of NSCLC A549 cells, induces activation of JNK signaling and triggers caspase cascade apoptosis mediated by the release of cytochrome *c*, which provides a better understanding of the molecular mechanisms of TSIIA on lung cancer.

Introduction

Tanshinone IIA (TSIIA, 1,6,6-trimethyl-6,7,8,9-tetrahydrophenanthro [1,2-b] furan-10,11-dione) is the most abundant diterpene quinine isolated from *Salvia miltiorrhiza*, known as 'Dan-Shen'. This plant has been safely used for more than 2,000 years in traditional Chinese medicine for treating a large variety of cardiovascular diseases including atherosclerosis, coronary artery disease, angina pectoris, myocardial infarction and hypertension (1). TSIIA and the other two tanshinones, cryptotanshinone (CTS) and tanshinone I (TSI), are the three major active ingredients, the potent antitumor properties of which have been extensively investigated both *in vitro* and *in vivo* in recent years (2). Previous studies have suggested that CTS mainly inhibited angiogenesis (3), while TSI mainly inhibited migration, invasion and metastasis (4). Whereas, TSIIA significantly induced cell apoptosis on a panel of human tumor cell lines, such as breast cancer (5-7), glioma (8), lung cancer (9,10), ovarian cancer (11), gastric cancer (12), hepatoma (13), leukemia (14), prostate cancer (15), renal cell carcinoma (16), cervix carcinoma (17) and colon cancer (18). Therefore, TSIIA might have therapeutic potential in cancer therapy. However, the molecular mechanisms of TSIIA-induced apoptosis still remain elusive.

Lung cancer is the leading cause of cancer mortality in USA and worldwide (19,20). It is estimated that about 585,720 Americans will die from cancer in 2014, corresponding to about 1,600 deaths per day with more than one-quarter due to lung cancer. Approximately 87% of lung cancer cases are non-small cell lung cancer (NSCLC) and the majority of patients presents with advanced stage disease at diagnosis (20,21). The available chemotherapeutics is often limited due to undesirable drug resistance and side-effects (22). The cell line A549 was first derived from the patient with lung cancer in 1972 (23). A549 cells are adenocarcinomic human alveolar basal epithelial cells, which were commonly employed as the *in vitro* model of NSCLC. In 2010, Chiu and Su showed that TSIIA induced apoptosis in A549 lung cancer cells *in vitro*, due to inducing the reactive oxygen species (ROS) release and upregulating the Bax/Bcl-2 ratio (9). In 2012, Liu *et al* demonstrated that TSIIA significantly inhibited tumor growth of A549 xenografts *in vivo* mediated by inhibiting NQO1, an emerging and promising therapeutic target in cancer therapy (24). As TSIIA exerted great antitumor activity in cellular and animal lung cancer models, it might be a promising new drug for the treatment of NSCLC.

Currently, three basic apoptotic signaling pathway have been established: mitochondria, endoplasmic reticulum, and death receptor, changes in which can provide rational targets for new anticancer drugs (25). Mitochondria could

Correspondence to: Professor Hong-Yu Liu, Department of Cardiovascular Surgery, The First Affiliated Hospital, Harbin Medical University, 199 Dazhi Street, Harbin 150001, P.R. China
E-mail: hyliu.hmu@gmail.com

Key words: tanshinone IIA, apoptosis, lung cancer, cytochrome *c*, caspase, JNK

be considered as a novel target for chemotherapies. A variety of key events in apoptosis focus on mitochondria, including the release of caspase activators (such as cytochrome *c*), changes in electron transport, loss of mitochondrial membrane potential, and participation of pro- and anti-apoptotic Bcl-2 family proteins (26). Furthermore, evidence suggests that the c-jun N-terminal kinase (JNK) cascade participates in the mitochondria-mediated death pathway in response to various chemical and physical stresses (27). The experiments related to some of these factors were carried out in this study. Our data demonstrate for the first time that TSIIA might induce the activation of JNK pathway, mediate the release of cytochrome *c*, and trigger the activation of caspase-9 and caspase-3 caspase cascade in the mitochondrial-induced apoptotic pathway.

Materials and methods

Chemicals and reagents. TSIIA (Fig. 1A, >97% HPLC) was purchased from Sigma-Aldrich Chemical Co. (Shanghai, China). A stock solution of 40 mM TSIIA was prepared in sterilized DMSO and further diluted to appropriate concentrations with cell culture medium immediately before use. DMSO [0.1% (v/v)] was used as a vehicle control throughout the study.

RPMI-1640 medium, heat-inactivated fetal bovine serum (FBS), penicillin and streptomycin were acquired from Gibco Co., USA. Cell Counting Kit-8 (CCK-8, #CK04) was obtained from Dojindo Laboratories (Kumamoto, Japan). Lactate dehydrogenase (LDH) assay kit (#A020) was purchased from Jiancheng Bioengineering Institute (Nanjing, China). JNK inhibitor SP600125 (#8177S) was purchased from Cell Signaling Technology (Danvers, MA). Hoechst Staining Kit (#C0003), Mito-Tracker Green (#C1048), Mitochondrial membrane potential assay kit with JC-1 (#C2006), Cell Mitochondria Isolation Kit (#C3601), Caspase-3 Activity Assay Kit (#C1115), Caspase-8 Activity Assay Kit (#C1151), Caspase-9 Activity Assay Kit (#C1157), BCA Protein Assay Kit (#P0012), BeyoECL Plus kit (#P0018), Alexa Fluor 555-labeled goat anti-mouse IgG (H+L) (#A0459), and all other antibodies for cytochrome *c*, Bax, β-actin, and goat anti-rabbit and anti-mouse secondary antibodies were purchased from Beyotime Institute of Biotechnology (Haimen, China). All other chemicals were of analytic grade and commercially available.

Cell culture. A549 human lung cancer cells were obtained from Cell Library of Committee on Type Culture Collection of Chinese Academy of Sciences. Cultures were maintained in 95% air and 5% CO_2 at 37˚C in RPMI-1640 with 10% FBS, 2 mM L-glutamine, 100 U/ml penicillin and 100 U/ml streptomycin. To determine the effects of JNK inhibitor (SP600125) on TSIIA-induced apoptosis in A549 cells, cell culture was pre-incubated for 2 h with SP600125 (10 μM) before the addition of TSIIA.

CCK-8 assay. A549 cells ($1x10^5$ cells/ml in 96-well culture plates) were treated with DMSO (0.1%) or TSIIA (2.5, 5, 10, 20 and 40 μM) for 48 h. The medium (90 μl) was incubated with 10 μl of CCK-8 solution for 2 h at 37˚C. Absorbance was read at 450 nm on a microplate reader (Bio-Rad Model 550, Bio-Rad Laboratories, Hercules, CA). Cell viability (%) was calculated as (experimental absorbance - background absorbance)/(control absorbance - background absorbance) x100% (28). IC_{50} value, the concentration of TSIIA inhibiting 50% of the cell growth at 48 h, was calculated by the method of Reed and Muench (29).

Clone formation assay. A549 cells seeded at 500 cells/well in 6-well culture plates were treated with DMSO (0.1%) or TSIIA (2.5, 5, 10, 20 and 40 μM) for 48 h and then maintained in the routine medium. After 10 days incubation, cell colonies consisting of more than 50 cells stained with crystal violet were counted and pictures were taken by a digital camera (30). The ratio of clone formation was calculated following the equation: rate of clone formation (%) = (clone amount/500) x100%. The IC_{50} value was then calculated.

LDH measurement. After A549 cells were exposed to DMSO (0.1%) or TSIIA (2.5, 5, 10, 20 and 40 μM) for 48 h, each culture medium was centrifuged at 250 x g for 10 min. Supernatant was transferred to a 96-well culture plate to determine the amount of LDH according to the manual of the LDH assay kit (31). LDH activity is reported as percentage relative to control level. Absorbance of samples was measured at 450 nm.

Detection of mitochondrial fluorescent. After treated with DMSO (0.1%) or TSIIA (20 μM) for 48 h, respectively, A549 cells were washed twice with pre-chilled PBS. The mitochondrial green fluorescent probe (Mito-Tracker Green) was added to a final concentration of 100 nm, and the cells were then cultured in the dark for 30 min (32). After being washed three times with PBS, the cells were imaged by a reflected fluorescence microscope (Nikon MF30 LED, Japan) with excitation wavelength of 490 nm and emission wavelength of 516 nm.

Measurement of mitochondrial membrane potential (MMP). After labeling cells using a Mito-Tracker Green, we measured the change in mitochondrial membrane potential of TSIIA-treated A549 cells. After treatment, cells were incubated with JC-1 (2.5 μg/ml) at 37˚C in dark for 20 min. After washing twice with ice-cold dyeing working buffer, the samples were collected and placed on ice using a method previously described (33). The MMP changes were evaluated by a FACSCalibur Flow Cytometer (Becton-Dickinson, San Jose, CA). High membrane potential was associated with emission at 590 nm (red), and low membrane potential at 530 nm (green) when excited at 488 nm. MMP was determined by a ratio of fluorescence intensity at 590 nm to that at 530 nm.

Immunofluorescent labeling. A549 cells were seeded on sterile cover glasses placed in the 6-well plates the day before treatment with DMSO (0.1%) or TSIIA (20 μM) for 48 h. After fixation with 4% formaldehyde, cells were permeabilized for 15 min in 1% Triton X-100 in PBS. The cells were incubated with the mouse anti-cytochrome *c* antibody overnight at 4˚C and then incubated with Alexa Fluor 555-labeled goat anti-mouse IgG (H+L) antibody for 2 h at room temperature. The nucleus was stained with Hoechst 33258 for 20 min in the dark (34). Images were observed under a reflected fluorescence microscope (Nikon MF30 LED, Japan).

Mitochondrial and cytosolic fractionation. After treatment with DMSO (0.1%) or TSIIA (20 μM) for 48 h, respectively, A549 cells were incubated in 100 μl ice-cold mitochondrial

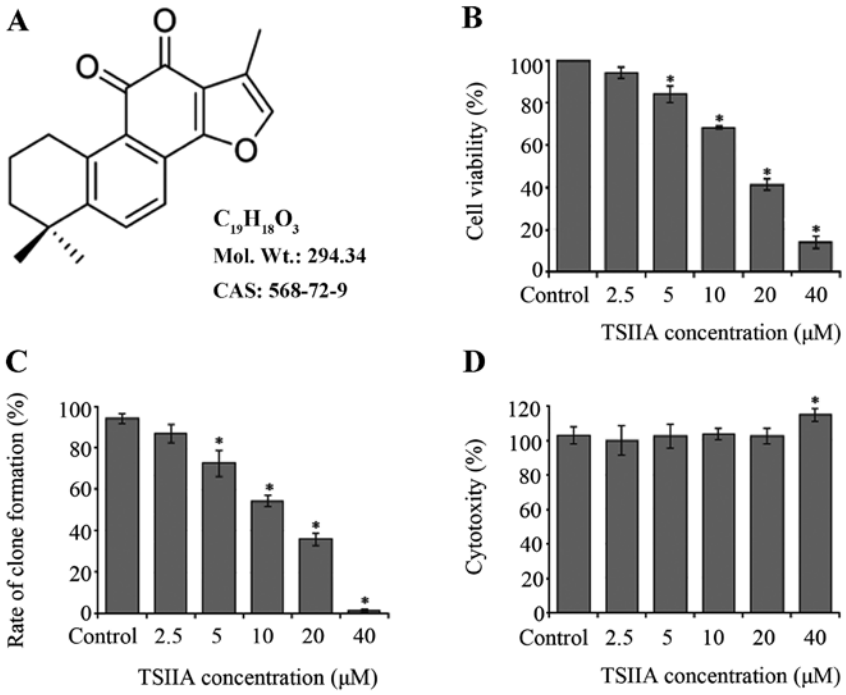

Figure 1. Effects of TSIIA on the growth of A549 cells. (A) Chemical structure of tanshinone IIA (TSIIA). (B) Cell viability (%) was determined by CCK-8 assay. Exponentially growing A549 cells were treated with the indicated concentration of TSIIA for 48 h. (C) Rate of clone formation (%) was determined by clone formation assay. (D) Cytotoxity (%) was determined by LDH measurement. Values are means ± SD (n=3). *p<0.05 vs. control.

lyses buffer on ice for 10 min. Cell suspension was then taken into a glass homogenizer and homogenized for 30 strokes using a tight pestle on ice. The homogenate was centrifuged at 600 x g for 10 min at 4˚C to remove nuclei and unbroken cells. Then the supernatant was collected and centrifuged again at 12,000 x g for 30 min at 4˚C to obtain the cytosol (supernatant) and mitochondria (deposition) fraction (35). Protein concentrations were determined using BCA Protein Assay Kit.

Western blot analysis. Release of cytochrome *c* from the mitochondria to cytosol and translocation of Bax from cytosol to mitochondria were measured by western blot analysis as previously described (36). The signal was visualized using a BeyoECL Plus kit. The level of β-actin was used to normalize the amount of the protein of interest. The density of the band was expressed relative to the density in vehicle control cells.

Caspase activity measurement. Lysates of A549 cells were prepared after treatment with TSIIA (10 or 20 μM) for 48 h. In some cases, cells were pretreated for 2 h with SP600125 (10 mM) before TSIIA treatment. Caspase-3, -8, -9 activity assays were performed on 96-well microplates by incubating 10 μl cell lysate in 80 μl reaction buffer containing 10 μl caspase substrate (2 mM). Lysates were incubated at 37˚C for 4 h. Samples were measured with a microplate reader at an absorbance of 405 nm. Caspase activity was expressed as the ratio of treated to vehicle control cells (37).

Statistical analysis. All data were obtained from three independent assays (n=3). Values were expressed as mean ± standard deviation (SD). Statistical analyses of the data between treated and control cells were performed by Student's t-test and one-way analysis of variance (ANOVA). A p-value <0.05 was considered statistically significant.

Results

TSIIA inhibits the proliferation of A549 cells. The number of viable cells was assessed by CCK-8 assay. Treatment with TSIIA (2.5, 5, 10, 20 and 40 μM) resulted in a dose-dependent suppression of cell viability (Fig. 1B, $p<0.05$). IC_{50} value of TSIIA on A549 cells was 16.0±3.7 μM at 48 h.

Also, clone formation assay was done to determine a long-term effect of TSIIA on A549 cell growth. The results of colony images showed that the rate of clone formation was reduced in a dose-dependent manner (Fig. 1C, $p<0.05$). IC_{50} value was 14.5±3.3 μM with 10 days incubation after TSIIA treatment for 48 h.

Leakage of LDH to the cell culture medium indicates cell membrane damage. Our LDH assay detects the amount of LDH released by cells with damaged membranes as indicator of necrosis. Except 40 μM, treatment with TSIIA (2.5, 5, 10 and 20) did not affect the concentration of LDH in the supernatant of culture medium (Fig. 1D, $p>0.05$). It suggested that the anti-proliferative effect of TSIIA on A549 cells was not due to cytotoxicity at the TSIIA dose of 10 and 20 μM, and these concentrations were used in further analysis.

TSIIA causes mitochondrial morphological changes and MMP loss. The change of mitochondrial morphology and decreasing of MMP are associated with mitochondrial damage linked to apoptosis (38). Thus, we next evaluated the effect of TSIIA on mitochondria. Cell shrinkage and cytoplasm vacuolization were observed in TSIIA-treated A549 cells (Fig. 2A and B).

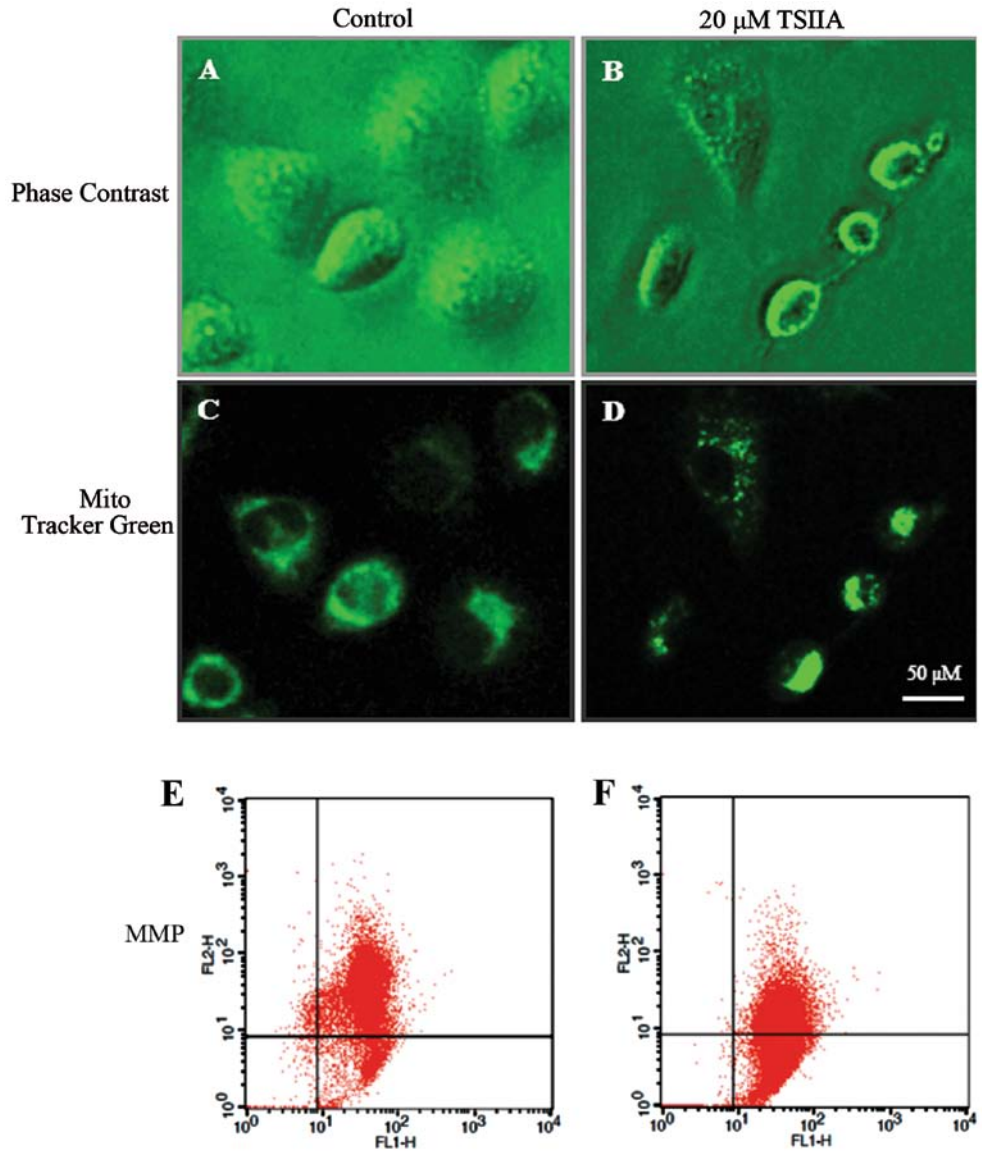

Figure 2. Mitochondrial morphological changes and MMP loss induced by TSIIA in A549 cells. Cells were treated with DMSO (0.1%) or TSIIA (20 μM) for 48 h and then observed under fluorescence microscopy (A, B, C and D) (magnification, x400). Scale bar, 50 μM. Pictures were enhances using Adobe Photoshop for brightness, contrast, and sharpening for uniformity of appearance only. Graphs of mitochondrial membrane potential (MMP) were evaluated by a FACSCalibur Flow Cytometer (E and F). Results were representative of three independent experiments.

As one of three results shown in Fig. 2D and F, after treatment with DMSO (0.1%) or TSIIA (20 μM), the JC-1 red/green fuorescent ratio in A549 cells was 5.83±0.862 and 1.14±0.156, respectively, suggesting that TSIIA induces a marked decrease of MMP in A549 cells ($p<0.05$). Compared to JC-1, the mitochondrial fluorescent probe Mito-Tracker Green, could track mitochondria independent of the MMP. It was observed that after TSIIA treatment, some mitochondria changed their filamentous staining pattern to aggregates, some lost the green fluorescence, which was different from the control group (Fig. 2C and D). As previous studies showed that TSIIA significantly induced cell apoptosis on a panel of human tumor cell lines, we thought that TSIIA could induce NSCLC A549 cell apoptosis through the mitochondria pathway.

TSIIA induces cytochrome c release into the cytosol and Bax translocation into mitochondria. The release of cytochrome *c* from mitochondria into the cytosol is one of the major apoptosis pathways (39). To elucidate whether cytochrome *c* release in TSIIA-induced apoptosis, we determined the subcellular localization of cytochrome *c* by immunofluorescent labeling. As shown in Fig. 3, the staining pattern became diffuse in most cells treated with 20 μM TSIIA for 48 h, consistent with a translocation of cytochrome *c* into the cytosol, whereas, cytochrome *c* displayed a dotted pattern in untreated cells, consistent with its location within the mitochondria. The condensation and fragmentation of the chromatin of the nucleus was also observed by Hoechst 33258 in these cells with diffuse cytochrome *c* staining.

It has been well documented that during mitochondria-mediated apoptosis, Bax can translocate from cytosol to mitochondria, causing the release of cytochrome *c* (40). By cell fractionation-based western blot assay, the results showed that Bax level reduced and cytochrome *c* level increased in the

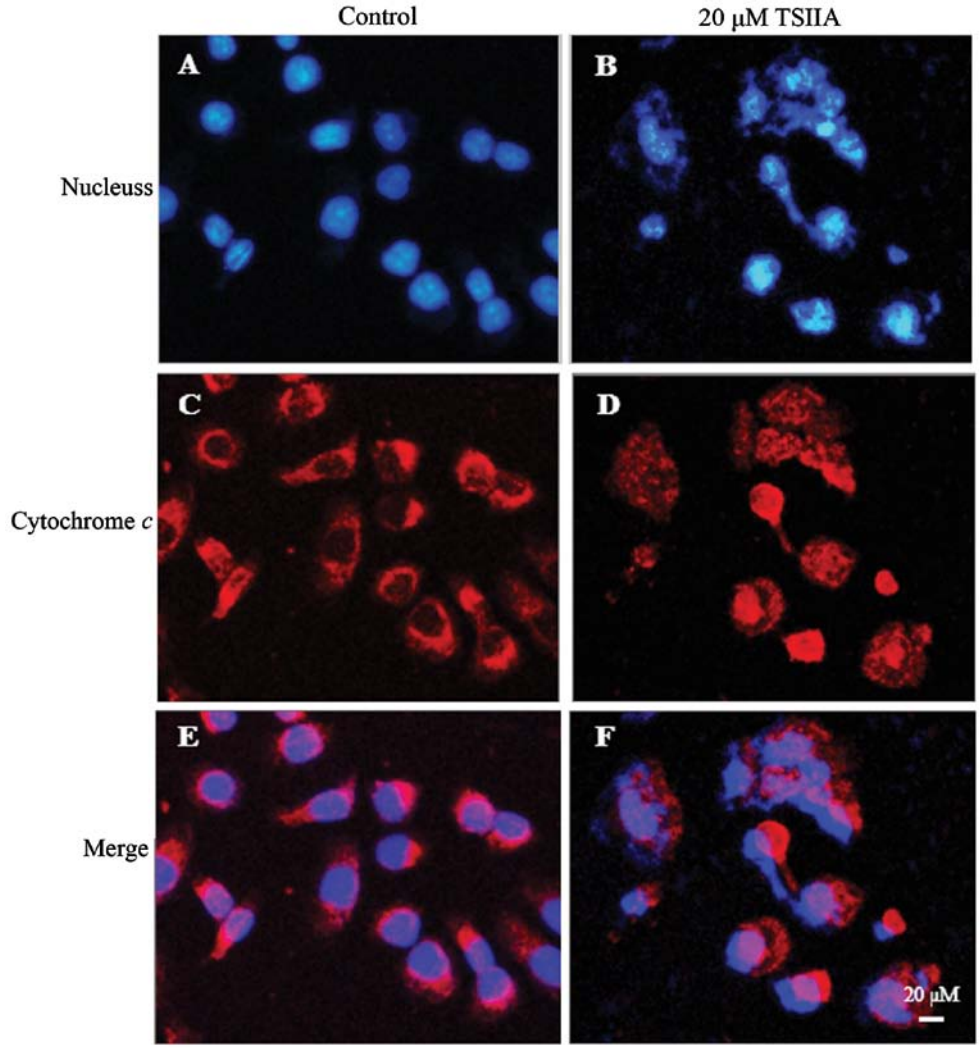

Figure 3. Effects of TSIIA on cytochrome *c* by cell immunofluorescence. A549 cells were treated with DMSO (0.1%) or TSIIA (20 μM) for 48 h and then images were taken with fluorescence microscopy (magnification, x200). Scale bar, 20 μM. (A and B) Nuclei (visualized with Hochest 33258, blue signal). (C and D) Localization of Alexa Fluor 555-Cyt *c* (Alexa Fluor 555 fluorescence, red signal). (E and F) Merge of the two images of (A and C) or (B and D), respectively. Results are representative of three independent experiments.

cytosol fraction, while Bax level increased and cytochrome *c* level decreased in the mitochondrial fraction in A549 cells treated with 20 μM TSIIA for 48 h (Fig. 5, $p<0.05$).

TSIIA activates the caspase-9 and caspase-3 cascade. The caspase cascade is crucial for apoptotic signal transduction. Cytosolic cytochrome *c* induces caspase-9-dependent activation of caspase-3 (41). The working principles of Caspase-3, -8 or -9 Activity Assay Kit are based on the cleavage of the following substrates: acetyl-Asp-Glu-Val-Asp p-nitroanilide (Ac-DEVD-pNA), acetyl-Ile-Glu-Thr-Asp p-nitroanilide (Ac-IETD-pNA) and acetyl-Leu-Glu-His-Asp p-nitroanilide (Ac-LEHD-pNA). Activity of caspase-9 and caspase-3 was shown to be dose-dependently increased with treatment of TSIIA for 48 h in A549 cells ($p<0.05$), but activity of caspase-8 was not significantly induced ($p>0.05$).

The JNK pathway plays a pivotal role in stress responses and induces apoptosis in response to various stimuli and the absence of JNK caused a defect in the mitochondrial death signaling pathway, including the failure to release cytochrome *c* (42). To detect whether TSIIA-induced mitochondria apoptosis related to JNK pathway, effects of SP600125 (10 μM, JNK inhibitor) on TSIIA-induced caspase activation were also assessed. The results showed that inhibition of JNK signaling by adding SP600125 significantly blocked caspase-9 and caspase-3 activation in A549 cells with TSIIA treatment (Fig. 5, $p<0.05$). This strongly suggested that JNK pathway performed a crucial function in TSIIA-induced apoptosis in A549 cells, accompanied by the activation of caspase-9 and caspase-3.

Discussion

TSIIA was originally isolated and identified from the traditional Chinese medicinal herb Dan-Shen. More than 40 tanshinones and their analogs have been isolated since the 1930s, which exhibit various biological activities of anti-atherosclerosis, cardioprotection, neuroprotection and antitumor effects (43). Studies in the past decade suggest that TSIIA hits the model of 'one-drug-multi-target-multi-disease', which is shared by traditional Chinese medicines (TCM), such as berberine (44). TSIIA

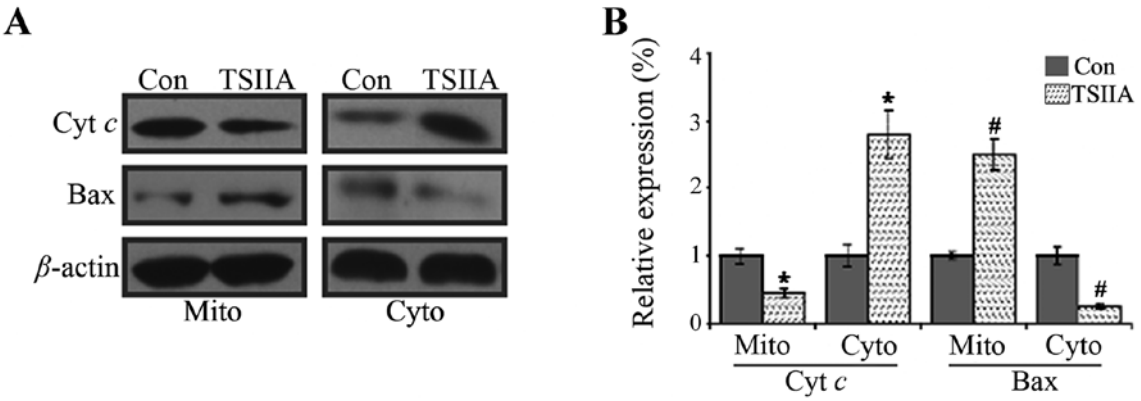

Figure 4. Effects of TSIIA on distribution and expression of Bax and cytochrome *c* (Cyt *c*). A549 cells were treated with DMSO (0.1%) or TSIIA (20 μM) for 48 h and protein expressions of Bax and Cyt *c* were tested by western blot analysis. Cyto, cytosole; Mito, mitochondria. β-actin was used as the internal control. Data are presented as means ± SD of three independent experiments and analyzed by one-way ANOVA. *p<0.05, Cyt *c* vs. control; $^{\#}$p<0.05, Bax vs. control.

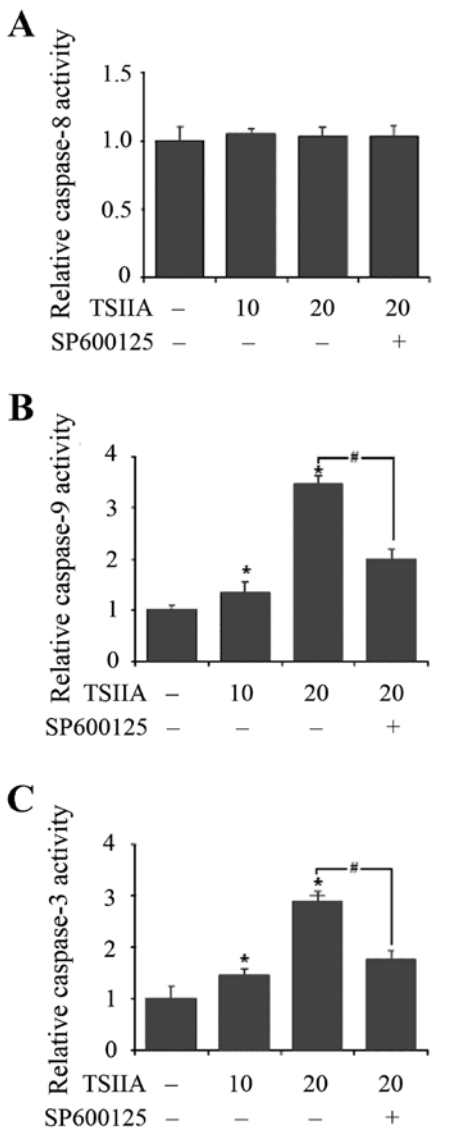

Figure 5. Effects of TSIIA on caspase-3, -8, -9 activation in A549 cells. Graphs were drawn from the results using (A) caspase-8, (B) caspase-9 and (C) caspase-3 Activity Assay kit. After various treatments as described in Materials and methods, activities of caspases were measured with a microplate reader at an absorbance of 405 nm. Values are means ± SD (n=3). *p<0.05 vs. control; $^{\#}$p<0.05 vs. 20 μM TSIIA-treated alone.

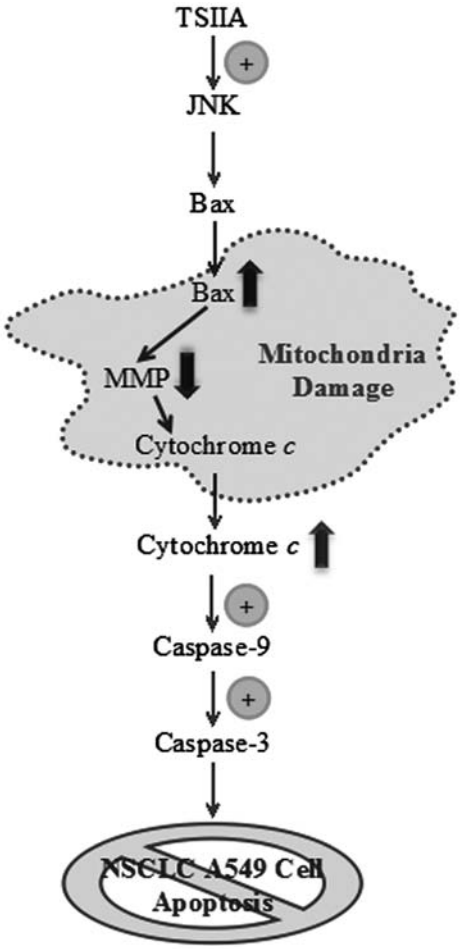

Figure 6. A proposed mechanism of TSIIA-induced apoptosis in A549 cells.

exhibited broad antitumor activity towards cancer cell lines of different origins, including H146 (10), A549 (9), COC1/DDP (11), BEL-7402 (13), U-937 (14), MDA-MB-231 (7), 786-O (16), LNCaP (15) and CaSki (17). However, the precise mechanism of the antitumor activity of TSIIA has remained unclear. For new drug development to treat human lung cancer, we evaluated the mechanism of apoptosis of TSIIA on NSCLC A549 cells *in vitro*.

Consistent with previous studies, the proliferation of A549 cells was significantly inhibited by exposure to various concentrations (2.5, 5, 10, 20 and 40 μM) of TSIIA in a dose-dependent manner by both CCK-8 assay (Fig. 1B) (9) and clone formation assay (Fig. 1C). The IC_{50} value (14.5±3.3 μM) obtained by clone formation assay was lower than that of CCK-8 assay (16.0±3.7 μM). In contrast to CCK-8 assay, clone formation is a very convenient and highly sensitive assay. With this long-term cell clonogenic ability assay, we revealed that TSIIA-treated A549 cells might perform an irreversible loss of long-term growth ability. Also, the results of LDH assay (Fig. 1D), show that the concentrations of TSIIA with 10 and 20 μM were without any obvious necrosis.

Mitochondria, which generate 80% of the energy required for cellular activities, are important sites of respiration and oxidative phosphorylation in the cell. To gain insight into the molecular mechanism involving TSIIA-induced apoptosis in A549 cells, some key factors in mitochondria-mediated apoptosis were assessed. MMP is an important parameter of mitochondrial function and has been used as an indicator of cell health. The loss of MMP is a hallmark for apoptosis (26). In this study, after 48 h with TSIIA (20 μM), the mitochondria morphological damage of A549 cells was present and the MMP was decreased (Fig. 2).

Accumulating evidence indicates that mechanism by which TSIIA induced apoptosis associated with expression of the Bcl-2 family proteins (9). We focused our efforts on one cardinal member of this family that are known to be pro-apoptotic Bax. In our study, Bax, localized in the outer mitochondrial membrane, was downregulated. This event might result in losing mitochondrial membrane potential and releasing cytochrome *c* from mitochondria into the cytosol, which can lead to irreversible commitment of A549 cells to apoptosis through the mitochondrial pathway (Figs. 3 and 4).

Furthermore, whether TSIIA could trigger apoptosis in the caspase cascade through the release of cytochrome *c*, activities of some important caspases were studied. Caspase-8 and caspase-9 are the key initiator caspases of the death receptor pathway and the mitochondrial pathway, respectively, that cleave and activate downstream effector caspases such as caspase-3 inducing apoptosis (26). Our results showed that TSIIA dose-dependently triggered the activity of caspase-3 and caspase-9 without significantly inducing the activity of caspase-8, which led to apoptosis in A549 cells through the mitochondrial pathway (Fig. 5).

Finally, we assessed whether TSIIA can induce apoptosis in the JNK-dependent pathway or the JNK-independent pathway. Previous research showed that Bax was essential for apoptotic signal transduction by JNK (45,46) and the release of cytochrome *c* from mitochondria was involved in apoptosis induced by JNK activation (42). We confirmed TSIIA induced apoptosis with cytochrome *c* release from mitochondria and Bax translocation to mitochondria. However, the relationship between TSIIA-induced apoptosis and JNK pathway has not been reported. In our study, SP600125, an inhibitor of JNK pathway, inhibited the TSIIA-induced activity of caspase-9 and caspase-3 (Fig. 5B and C). Although our present data did not confirm whether another pathway performed this function, our findings here indicated that in response to TSIIA, the JNK pathway might give rise to apoptosis of A549 cells.

Altogether these studies revealed for the first time a regulatory mechanism of TSIIA-induced apoptosis, which was associated, at least in part, with the activation of JNK signaling and caspase cascade mediated by the release of cytochrome *c* (Fig. 6). Given the fact that TSIIA has been safely used in the clinic (mostly in China) (2,47), TSIIA may be a novel therapeutic for treating NSCLC.

Acknowledgements

This study was supported by the research fund of Harbin Medical University, P.R. China.

References

1. Xu S and Liu P: Tanshinone II-A: new perspectives for old remedies. Expert Opin Ther Pat 23: 149-153, 2013.
2. Tian XH and Wu JH: Tanshinone derivatives: a patent review (January 2006 - September 2012). Expert Opin Ther Pat 23: 19-29, 2013.
3. Hur JM, Shim JS, Jung HJ and Kwon HJ: Cryptotanshinone but not tanshinone IIA inhibits angiogenesis in vitro. Exp Mol Med 37: 133-137, 2005.
4. Lee CY, Sher HF, Chen HW, *et al*: Anticancer effects of tanshinone I in human non-small cell lung cancer. Mol Cancer Ther 7: 3527-3538, 2008.
5. Wang X, Wei Y, Yuan S, *et al*: Potential anticancer activity of tanshinone IIA against human breast cancer. Int J Cancer 116: 799-807, 2005.
6. Lu Q, Zhang P, Zhang X and Chen J: Experimental study of the anticancer mechanism of tanshinone IIA against human breast cancer. Int J Mol Med 24: 773-780, 2009.
7. Su CC, Chien SY, Kuo SJ, Chen YL, Cheng CY and Chen DR: Tanshinone IIA inhibits human breast cancer MDA-MB-231 cells by decreasing LC3-II, Erb-B2 and NF-κBp65. Mol Med Rep 5: 1019-1022, 2012.
8. Wang J, Wang X, Jiang S, *et al*: Growth inhibition and induction of apoptosis and differentiation of tanshinone IIA in human glioma cells. J Neurooncol 82: 11-21, 2007.
9. Chiu TL and Su CC: Tanshinone IIA induces apoptosis in human lung cancer A549 cells through the induction of reactive oxygen species and decreasing the mitochondrial membrane potential. Int J Mol Med 25: 231-236, 2010.
10. Cheng CY and Su CC: Tanshinone IIA may inhibit the growth of small cell lung cancer H146 cells by upregulating the Bax/Bcl-2 ratio and decreasing mitochondrial membrane potential. Mol Med Rep 3: 645-650, 2010.
11. Jiao JW and Wen F: Tanshinone IIA acts via p38 MAPK to induce apoptosis and the downregulation of ERCC1 and lung-resistance protein in cisplatin-resistant ovarian cancer cells. Oncol Rep 25: 781-788, 2011.
12. Chen J, Shi DY, Liu SL and Zhong L: Tanshinone IIA induces growth inhibition and apoptosis in gastric cancer *in vitro* and *in vivo*. Oncol Rep 27: 523-528, 2012.
13. Dai ZK, Qin JK, Huang JE, *et al*: Tanshinone IIA activates calcium-dependent apoptosis signaling pathway in human hepatoma cells. J Nat Med 66: 192-201, 2012.
14. Liu C, Li J, Wang L, *et al*: Analysis of tanshinone IIA induced cellular apoptosis in leukemia cells by genome-wide expression profiling. BMC Complement Altern Med 12: 5, 2012.
15. Won SH, Lee HJ, Jeong SJ, Lu J and Kim SH: Activation of p53 signaling and inhibition of androgen receptor mediate tanshinone IIA induced G1 arrest in LNCaP prostate cancer cells. Phytother Res 26: 669-674, 2012.
16. Wei X, Zhou L, Hu L and Huang Y: Tanshinone IIA arrests cell cycle and induces apoptosis in 786-O human renal cell carcinoma cells. Oncol Lett 3: 1144-1148, 2012.
17. Pan TL, Wang PW, Hung YC, Huang CH and Rau KM: Proteomic analysis reveals tanshinone IIA enhances apoptosis of advanced cervix carcinoma CaSki cells through mitochondria intrinsic and endoplasmic reticulum stress pathways. Proteomics 13: 3411-3423, 2013.

18. Liu M, Wang Q, Liu F, *et al*: UDP-glucuronosyltransferase 1A compromises intracellular accumulation and anti-cancer effect of tanshinone IIA in human colon cancer cells. PLoS One 8: e79172, 2013.
19. Jemal A, Bray F, Center MM, Ferlay J, Ward E and Forman D: Global cancer statistics. CA Cancer J Clin 61: 69-90, 2011.
20. Siegel R, Ma J, Zou Z and Jemal A: Cancer statistics, 2014. CA Cancer J Clin 64: 9-29, 2014.
21. Novello S, Milella M, Tiseo M, *et al*: Maintenance therapy in NSCLC: why? To whom? Which agent? J Exp Clin Cancer Res 30: 50, 2011.
22. Wu CP, Ohnuma S and Ambudkar SV: Discovering natural product modulators to overcome multidrug resistance in cancer chemotherapy. Curr Pharm Biotechnol 12: 609-620, 2011.
23. Giard DJ, Aaronson SA, Todaro GJ, *et al*: In vitro cultivation of human tumors: establishment of cell lines derived from a series of solid tumors. J Natl Cancer Inst 51: 1417-1423, 1973.
24. Liu F, Yu G, Wang G, *et al*: An NQO1-initiated and p53-independent apoptotic pathway determines the anti-tumor effect of tanshinone IIA against non-small cell lung cancer. PLoS One 7: e42138, 2012.
25. Danial NN and Korsmeyer SJ: Cell death: critical control points. Cell 116: 205-219, 2004.
26. Green DR and Reed JC: Mitochondria and apoptosis. Science 281: 1309-1312, 1998.
27. Davis RJ: Signal transduction by the JNK group of MAP kinases. Cell 103: 239-252, 2000.
28. Wen M, Wang H, Zhang X, *et al*: Cytokine-like 1 is involved in the growth and metastasis of neuroblastoma cells. Int J Oncol 41: 1419-1424, 2012.
29. Devignat R: Calculation of Reed and Muench's 50 percent point in survival time measured in a recording cage. Ann Inst Pasteur (Paris) 83: 372-380, 1952.
30. Franken NA, Rodermond HM, Stap J, *et al*: Clonogenic assay of cells in vitro. Nat Protoc 1: 2315-2319, 2006.
31. Huang CC, Aronstam RS, Chen DR and Huang YW: Oxidative stress, calcium homeostasis, and altered gene expression in human lung epithelial cells exposed to ZnO nanoparticles. Toxicol In Vitro 24: 45-55, 2010.
32. Xu F, Yu H, Liu J and Cheng L: Pyrroloquinoline quinone inhibits oxygen/glucose deprivation-induced apoptosis by activating the PI3K/AKT pathway in cardiomyocytes. Mol Cell Biochem 386: 107-115, 2014.
33. Zhao J, Chen X, Lin W, *et al*: Total alkaloids of *Rubus aleaefolius* Poir inhibit hepatocellular carcinoma growth *in vivo* and *in vitro* via activation of mitochondrial-dependent apoptosis. Int J Oncol 42: 971-978, 2013.
34. Gao LW, Zhang J, Yang WH, Wang B and Wang JW: Glaucocalyxin A induces apoptosis in human leukemia HL-60 cells through mitochondria-mediated death pathway. Toxicol In Vitro 25: 51-63, 2011.
35. Zhang Z, Wang S, Qiu H, Duan C and Ding K and Wang Z: Waltonitone induces human hepatocellular carcinoma cells apoptosis in vitro and in vivo. Cancer Lett 286: 223-231, 2009.
36. Viedma-Rodriguez R, Baiza-Gutman LA, Garcia-Carranca A, Moreno-Fierros L, Salamanca-Gomez F and Arenas-Aranda D: Suppression of the death gene BIK is a critical factor for resistance to tamoxifen in MCF-7 breast cancer cells. Int J Oncol 43: 1777-1786, 2013.
37. Zhao D, Lin F, Wu X, *et al*: Pseudolaric acid B induces apoptosis via proteasome-mediated Bcl-2 degradation in hormone-refractory prostate cancer DU145 cells. Toxicol In Vitro 26: 595-602, 2012.
38. Chipuk JE, Bouchier-Hayes L and Green DR: Mitochondrial outer membrane permeabilization during apoptosis: the innocent bystander scenario. Cell Death Differ 13: 1396-1402, 2006.
39. Newmeyer DD and Ferguson-Miller S: Mitochondria: releasing power for life and unleashing the machineries of death. Cell 112: 481-490, 2003.
40. Finucane DM, Bossy-Wetzel E, Waterhouse NJ, Cotter TG and Green DR: Bax-induced caspase activation and apoptosis via cytochrome c release from mitochondria is inhibitable by Bcl-xL. J Biol Chem 274: 2225-2233, 1999.
41. Budihardjo I, Oliver H, Lutter M, *et al*: Biochemical pathways of caspase activation during apoptosis. Annu Rev Cell Dev Biol 15: 269-290, 1999.
42. Tournier C, Hess P, Yang DD, *et al*: Requirement of JNK for stress-induced activation of the cytochrome c-mediated death pathway. Science 288: 870-874, 2000.
43. Dong Y, Morris-Natschke SL and Lee KH: Biosynthesis, total syntheses, and antitumor activity of tanshinones and their analogs as potential therapeutic agents. Nat Prod Rep 28: 529-542, 2011.
44. Tillhon M, Guaman Ortiz LM, Lombardi P and Scovassi AI: Berberine: new perspectives for old remedies. Biochem Pharmacol 84: 1260-1267, 2012.
45. Tsuruta F, Sunayama J, Mori Y, *et al*: JNK promotes Bax translocation to mitochondria through phosphorylation of 14-3-3 proteins. EMBO J 23: 1889-1899, 2004.
46. Lei K, Nimnual A, Zong WX, *et al*: The Bax subfamily of Bcl2-related proteins is essential for apoptotic signal transduction by c-Jun NH(2)-terminal kinase. Mol Cell Biol 22: 4929-4942, 2002.
47. Bi HC, Zuo Z, Chen X, *et al*: Preclinical factors affecting the pharmacokinetic behaviour of tanshinone IIA, an investigational new drug isolated from *Salvia miltiorrhiza* for the treatment of ischaemic heart diseases. Xenobiotica 38: 185-222, 2008.